ELSEVIER

Available online at www.sciencedirect.com

SCIENCE DIRECT®

Journal of Computational and Applied Mathematics 168 (2004) 425–435

JOURNAL OF COMPUTATIONAL AND APPLIED MATHEMATICS

www.elsevier.com/locate/cam

Flux limiters in the coupling of radiation and hydrodynamic models☆

M. Seaïd[a,*], A. Klar[a], B. Dubroca[b]

[a] *Fachbereich Mathematik, TU Darmstadt, Darmstadt 64289, Germany*
[b] *CEA/CESTA BP 233114 Le Barp Cedex, France*

Received 16 September 2002; received in revised form 19 June 2003

Abstract

Two numerical approximations to radiative heat transfer problem based on asymptotic and entropy approaches are proposed for hydrodynamics radiation coupling. We compare the radiative fluxes between the two approaches and we show that the coupling based on the entropy approach is flux limited, while the other approach does not preserve this condition. Relaxation schemes are considered for the hydrodynamic part, and an iterative procedure is used for radiation. The new splitting algorithm avoids the use of Riemann solvers and Newton iterations. Numerical examples are carried out on two and three dimensional problems.

Keywords: Hydrodynamics; Radiation; Relaxation schemes; Iterative methods

1. Introduction

The problem of coupling the radiative transfer to hydrodynamics has been an immensely challenging one in the general areas of computational astrophysics, laser fusion and combustion phenomena, see [2,10] and further references are therein. Indeed, the equations governing this problem are strongly coupled due to the interaction between fluid dynamics, transport, and radiative heat transfer. Moreover, as a result of the dependence of radiation energy on the temperature, these equations are highly nonlinear. Furthermore, it is well known that the solutions of these equations are characterized by steep fronts, sharp peaks and even shock discontinuities, which need to be resolved accurately in applications and often cause severe numerical difficulties. Finally, the large number of

☆ This work was supported by the German research foundation SFB 568.
* Corresponding author.
E-mail address: seaid@mathematik.tu-darmstadt.de (M. Seaïd).

0377-0427/$ - see front matter
doi:10.1016/j.cam.2003.06.014

unknowns, the difference on propagation between radiative signals and hydrodynamic flows, and the computational cost are typical difficulties in radiation hydrodynamic computations. Hence, it is the purpose of the present work to derive a numerical model for radiation hydrodynamics that offers the following properties:

- The model used to approach the full radiative transfer equation should preserve the physical features of the full equation, for instance, the radiative flux must be limited by the light speed i.e. any radiative signal has a velocity below the light speed. In this paper we propose two approaches to the radiative transfer equation. The P_1 approach [10] based on asymptotic analysis and the M_1 approach [9] based on entropy principle. Numerical examples presented here show that coupling the hydrodynamic to M_1 approach preserves the flux-limited property, whereas the other coupling does not.
- The numerical methods used to compute the solution of the coupling model should resolve and keep track of shocks involved and at the same time treat the radiation signals efficiently. In this paper we introduce a two stages splitting technique. The hydrodynamic stage of the splitting is straightforwardly treated by a high resolution scheme, while the radiative stage uses a monotone iterative method. The new algorithm is second order in space and time, robust and avoids the use of Riemann solvers and Newton iterations.

The plan of this paper is as follows. In Section 2 radiation hydrodynamic equations are formulated. The numerical procedure for the hydrodynamic stage of the splitting is presented in Section 3. Section 4 is devoted to the numerical procedure for the radiation stage. Numerical tests validating our approximations are given in Section 5. Section 6 contains the conclusion.

2. Governing equations

The radiation hydrodynamic equations we consider in this paper can be written as a hyperbolic system of conservation laws for gas material together with emission and absorption of radiation. If we assume that the gas material is radiatively opaque i.e., the mean-free-path of photons is much smaller than the typical length of flows, and the absorption coefficient is independent of the frequency. Then, after neglecting the scattering effects, the radiation hydrodynamic equations are written in dimensionless form as follows

$$\partial_t \rho + \nabla \cdot (\rho \mathbf{u}) = 0,$$

$$\partial_t \rho \mathbf{u} + \nabla \cdot (\rho(\mathbf{u} \otimes \mathbf{u}) + p) = 0,$$

$$\partial_t E + \nabla \cdot (\mathbf{u}(E + p)) = \nabla \cdot (\lambda \nabla T) - \sigma(4\pi B(T) - \varphi). \tag{1}$$

ρ, $\mathbf{u} = (u_1, u_2, u_3)^{\mathrm{T}}$, p, E, T and φ denote, respectively, the mass density, the flow velocity, the thermal pressure, the total energy, the temperature and the radiative energy. In the above and in what follows bold face type denote vector quantities. The equation of state

$$p = R\rho T = (\gamma - 1)\left(E - \frac{\rho}{2}\mathbf{u}^2\right), \tag{2}$$

is required, where R is the gas constant and γ is the specific heat ratio. λ and σ denote respectively, the heat conductivity and the absorption coefficients. The function $B(T) = a_R T^4$, with a_R is the radiation constant.

To close the system (1) an equation for the radiative energy is needed. For this end we consider two approaches

The well known P_1 approximation [7,10] given by

$$\nabla \cdot \left(\frac{-1}{3\sigma} \nabla \varphi \right) + \sigma \varphi = 4\pi\sigma B(T). \tag{3}$$

The M_1 approximation studied in [5,9] as

$$\nabla \cdot \mathbf{\Psi} + \sigma \varphi = 4\pi\sigma B(T),$$

$$\nabla \cdot (\mathbf{D}\varphi) + \sigma \mathbf{\Psi} = 0, \tag{4}$$

where the Eddington tensor $\mathbf{D}$ is defined as

$$\mathbf{D} = \frac{1-\chi}{2}\mathbf{I} + \frac{3\chi - 1}{2}\frac{\mathbf{f} \otimes \mathbf{f}}{\|\mathbf{f}\|^2}, \quad \text{with } \mathbf{f} = \frac{\mathbf{\Psi}}{\varphi}, \quad \text{and} \quad \chi = \frac{3 + 4\|\mathbf{f}\|^2}{5 + 2\sqrt{4 - 3\|\mathbf{f}\|^2}}.$$

Note that if we set $\mathbf{D} = \frac{1}{3}\mathbf{I}$, where $\mathbf{I}$ is the identity matrix, then Eqs. (4) are reduced to the P_1 model (3). Henceforth we term $\mathscr{P}_1$ to Eqs. (1)–(3) and $\mathscr{M}_1$ to Eqs. (1)–(4), and we define its associated radiative fluxes as

$$\mathbf{f}_{\mathscr{P}_1} = \frac{-1}{3\sigma}\nabla\varphi, \quad \text{and} \quad \mathbf{f}_{\mathscr{M}_1} = \frac{\mathbf{\Psi}}{\varphi}, \tag{5}$$

and the normalized fluxes are $\tilde{\mathbf{f}}_{\mathscr{P}_1} = \mathbf{f}_{\mathscr{P}_1}/c$, $\tilde{\mathbf{f}}_{\mathscr{M}_1} = \mathbf{f}_{\mathscr{M}_1}/c$, where c is the light speed in the vacuum. As will be shown in Section 4, it is important to note that $\tilde{\mathbf{f}}_{\mathscr{M}_1}$ is bounded below one ($\|\tilde{\mathbf{f}}_{\mathscr{M}_1}\| \leqslant 1$). This limitation is not satisfied by $\tilde{\mathbf{f}}_{\mathscr{P}_1}$.

Notice that in (1) we have assumed the thermodynamic equilibrium, i.e., the radiative and the fluid temperatures are equal. Furthermore, the models $\mathscr{P}_1$ and $\mathscr{M}_1$ are defined in a space domain Ω, time interval $[0, T]$ and subject to appropriate boundary and initial conditions.

A natural way to approximate solutions to $\mathscr{P}_1$ or $\mathscr{M}_1$ consists of splitting the set of Eqs. (1)–(3) or (1)–(4) in the two following sets of equations

$$\partial_t \mathbf{U} + \partial_x \mathbf{F}(\mathbf{U}) + \partial_y \mathbf{G}(\mathbf{U}) + \partial_z \mathbf{H}(\mathbf{U}) = 0, \tag{6}$$

for hydrodynamic and

$$\partial_t E - \nabla \cdot (\lambda \nabla T) = -\sigma(4\pi B(T) - \varphi),$$

$$-\nabla \cdot \left(\frac{1}{3\sigma}\nabla\varphi \right) = \sigma(4\pi B(T) - \varphi), \tag{7}$$

for $\mathscr{P}_1$ or

$$\partial_t E - \nabla \cdot (\lambda \nabla T) = -\sigma(4\pi B(T) - \varphi),$$

$$\nabla \cdot \mathbf{\Psi} = \sigma(4\pi B(T) - \varphi),$$

$$\nabla(\mathbf{D}\varphi) = -\sigma \mathbf{\Psi}, \tag{8}$$

for $\mathscr{M}_1$. Here

$$\mathbf{U} = \begin{pmatrix} \rho \\ \rho u_1 \\ \rho u_2 \\ \rho u_3 \\ E \end{pmatrix}, \quad \mathbf{F} = \begin{pmatrix} \rho u_1 \\ \rho u_1^2 + p \\ \rho u_1 u_2 \\ \rho u_1 u_3 \\ u_1(E+p) \end{pmatrix}, \quad \mathbf{G} = \begin{pmatrix} \rho u_2 \\ \rho u_1 u_2 \\ \rho u_2^2 + p \\ \rho u_2 u_3 \\ u_2(E+p) \end{pmatrix}, \quad \mathbf{H} = \begin{pmatrix} \rho u_3 \\ \rho u_1 u_3 \\ \rho u_2 u_3 \\ \rho u_3^2 + p \\ u_3(E+p) \end{pmatrix}.$$

Numerically, we solve the $\mathscr{P}_1$ or $\mathscr{M}_1$ model through consecutively solving Eq. (6). The total energy obtained through solving (6) is only an intermediate solution, which should be updated through Eqs. (7) for $\mathscr{P}_1$ model or (8) for $\mathscr{M}_1$ model.

3. Numerical procedure: hydrodynamics

For simplicity in formulation, we consider only the two-dimensional case of (1), and the extension to the three-dimensional case is straightforward. To discretize in space, we cover Ω by the numerical nonuniform grids

$$\{(x_i,\ y_j)^{\mathrm{T}},\ x_i = ih_i,\ y_j = jh_j,\ i = 1,2\ldots,\ Nx,\ j = 1,2\ldots,Ny\}.$$

We use the notations

$$\omega_{ij} = \frac{1}{h_i h_j} \int_{x_{i-1/2}}^{x_{i+1/2}} \int_{y_{i-1/2}}^{y_{i+1/2}} \omega(x,y)\,\mathrm{d}x\mathrm{d}y, \quad \text{and} \quad \omega_{i+(1/2)j+(1/2)} = \omega(x_{i+1/2}, y_{j+1/2}).$$

We define the following difference operators

$$\mathscr{D}_x \omega_{ij} = \frac{\omega_{i+(1/2)j} - \omega_{i-(1/2)j}}{h_i}, \quad \mathscr{D}_y \omega_{ij} = \frac{\omega_{ij+1/2} - \omega_{ij-1/2}}{h_j}. \tag{9}$$

Then, a semi-discrete approximation for (6) can be directly written as

$$\frac{\mathrm{d}\mathbf{U}_{ij}}{\mathrm{d}t} + \mathscr{D}_x \mathbf{V}_{ij}|_{\mathbf{V}_{ij}=F(\mathbf{U}_{ij})} + \mathscr{D}_y \mathbf{W}_{ij}|_{\mathbf{W}_{ij}=G(\mathbf{U}_{ij})} = 0, \tag{10}$$

where the numerical fluxes are given for the kth component ($k = 1,2,3,4$) by

$$U_{i+(1/2)j} = \frac{U_{ij} + U_{i+1j}}{2} - \frac{V_{i+1j} - V_{ij}}{2\lambda_k} + \frac{\sigma_{ij}^{x,+} + \sigma_{i+1j}^{x,-}}{4\lambda_k},$$

$$V_{i+(1/2)j} = \frac{V_{ij} + V_{i+1j}}{2} - \lambda_k \frac{U_{i+1j} - U_{ij}}{2} + \frac{\sigma_{ij}^{x,+} - \sigma_{i+1j}^{x,-}}{4},$$

$$U_{ij+1/2} = \frac{U_{ij} + U_{ij+1}}{2} - \frac{W_{ij+1} - W_{ij}}{2\mu_k} + \frac{\sigma_{ij}^{y,+} + \sigma_{ij+1}^{y,-}}{4\mu_k},$$

$$W_{ij+1/2} = \frac{W_{ij} + W_{ij+1}}{2} - \mu_k \frac{U_{ij+1} - U_{ij}}{2} + \frac{\sigma_{ij}^{y,+} - \sigma_{ij+1}^{y,-}}{4}.$$

λ_k and μ_k are given by the kth eigenvalue of the Jacobian matrix $\partial\mathbf{F}/\partial\mathbf{U}$ and $\partial\mathbf{G}/\partial\mathbf{U}$, respectively: $\lambda_1 = |u - c_s|$, $\lambda_2 = \lambda_3 = u$, $\lambda_4 = u + c_s$ and $\mu_1 = |v - c_s|$, $\mu_2 = \mu_3 = v$ and $\mu_4 = v + c_s$. The sound speed c_s is defined by $c_s^2 = \gamma p/\rho$. The slope limiters are defined as

$$\sigma_{ij}^{x,\pm} = (V_{i+1j} \pm \lambda_k U_{i+1j} - V_{ij} \mp \lambda_k U_{ij})\phi(\theta_{ij}^{x,\pm}),$$

$$\theta_{ij}^{x,\pm} = \frac{V_{ij} \pm \lambda_k U_{ij} - V_{i-1j} \mp \lambda_k U_{i-1j}}{V_{i+1j} \pm \lambda_k U_{i+1j} - V_{ij} \mp \lambda_k U_{ij}},$$

$$\sigma_{ij}^{y,\pm} = (W_{ij+1} \pm \mu_k U_{ij+1} - W_{ij} \mp \mu_k U_{ij})\phi(\theta_{ij}^{y,\pm}),$$

$$\theta_{ij}^{y,\pm} = \frac{W_{ij} \pm \mu_k U_{ij} - W_{ij-1} \mp \mu_k U_{ij-1}}{W_{ij+1} \pm \mu_k U_{ij+1} - W_{ij} \mp \mu_k U_{ij}}.$$

For the slope limiter function ϕ we used the Van Leer limiter function [8]. In principle, the above space discretization is based on combining the second order MUSCL method [8] with the relaxation scheme [6], which the authors referred to as relaxed scheme. The main advantage of considering such a method is that no Riemann solvers are involved during the discretization.

The time integration of the semi-discrete equations (10) may be handled by any implicit ode's solver, since they are computationally without risk by virtue of their accuracy and linear unconditionally stability. This allows for larger time steps in the integration process. However, due to the large set of nonlinear algebraic equations at each time step, these methods may be quite slow. In this section we use the modified three-stages second order explicit Runge–Kutta scheme introduced in [1]. It is shown that the scheme is I-stable and possess a large stability region over the classical second order Runge–Kutta method.

Let the time interval $[0, T]$ be divided into subintervals $[t_n, t_{n+1}]$ of length Δt such that $t_n = n\Delta t$, we denote $\omega_{ij,n} = \omega_{ij}(t_n)$. Hence, the implementation of the hydrodynamic algorithm to solve (6) is carried out in the following simple steps: Given $\mathbf{U}_{ij,n}$, $\mathbf{U}_{ij,n+1}$ is computed by

$$\mathbf{U}_{ij}^{(1)} = \mathbf{U}_{ij,n} - \frac{\Delta t}{3}(\mathscr{D}_x \mathbf{V}_{ij,n}|_{\mathbf{V}_{ij,n}=\mathbf{F}(\mathbf{U}_{ij,n})} + \mathscr{D}_y \mathbf{W}_{ij,n}|_{\mathbf{W}_{ij,n}=\mathbf{G}(\mathbf{U}_{ij,n})}),$$

$$\mathbf{U}_{ij}^{(2)} = \mathbf{U}_{ij,n} - \frac{\Delta t}{2}(\mathscr{D}_x \mathbf{V}_{ij}^{(1)}|_{\mathbf{V}_{ij}^{(1)}=\mathbf{F}(\mathbf{U}_{ij}^{(1)})} + \mathscr{D}_y \mathbf{W}_{ij}^{(1)}|_{\mathbf{W}_{ij}^{(1)}=\mathbf{G}(\mathbf{U}_{ij}^{(1)})}),$$

$$\mathbf{U}_{ij}^{(3)} = \mathbf{U}_{ij,n} - \Delta t(\mathscr{D}_x \mathbf{V}_{ij}^{(2)}|_{\mathbf{V}_{ij}^{(2)}=\mathbf{F}(\mathbf{U}_{ij}^{(2)})} + \mathscr{D}_y \mathbf{W}_{ij}^{(2)}|_{\mathbf{W}_{ij}^{(2)}=\mathbf{G}(\mathbf{U}_{ij}^{(2)})}),$$

$$\mathbf{U}_{ij,n+1} = \mathbf{U}_{ij}^{(3)}. \tag{11}$$

Notice that, the new solution vector $\mathbf{U}_{ij,n+1}$ computed by (11) contains, density, moments and energy at the new time level t_{n+1}. To update the pressure we used the state equation (2). Moreover, using the hydrodynamic approach (10)–(11) neither linear algebraic equation nor nonlinear source terms can arise. In addition the algorithm is TVD, stable under the usual CFL condition and second order accurate in space and time.

4. Numerical procedure: radiation

Unlike the hydrodynamic stage where much care must be given to the space discretization and explicit schemes to resolve the shocks accurately, in the radiative stage of the splitting, attention is given to time integration and implicit schemes. Since the hydrodynamic solution $\mathbf{U}$ has been updated through the first stage of the splitting (6), the second stage of the splitting is used to update the total energy E and therefore the temperature T together with the radiative energy φ. Therefore, for $\mathscr{P}_1$ model, we write Eqs. (7) as

$$\begin{aligned}
&\partial_t \tilde{E} - \nabla\cdot(\lambda\nabla T) = -\sigma(4\pi B(T) - \varphi),\\
&-\nabla\cdot\left(\frac{1}{3\sigma}\nabla\varphi\right) = \sigma(4\pi B(T) - \varphi),
\end{aligned} \tag{12}$$

where $\tilde{E}$ is the part of energy depending on temperature, $\tilde{E} = R\rho T/(\gamma - 1)$.

In order to maintain the same order of accuracy as in the hydrodynamic stage, we use the Crank–Nicolson method to integrate in time (12) along with the monotone iterations [11]. Hence, using the same notations as in the previous section, Eqs. (12) transform to

$$\begin{aligned}
&T^{(0)}_{ij,n+1} = T_{ij,n}, \quad \varphi^{(0)}_{ij,n+1} = \varphi_{ij,n},\\
&-\mathscr{D}_h^2\left(\frac{\Delta t\lambda}{2}T^{(m+1)}_{n+1}\right)_{ij} + \frac{R\rho}{\gamma-1}T^{(m+1)}_{ij,n+1} + \Gamma_1 T^{(m+1)}_{ij,n+1} = \Gamma_1 T^{(m)}_{ij,n+1} + F_1,\\
&-\mathscr{D}_h^2\left(\frac{1}{3\sigma}\varphi^{(m+1)}_{n+1}\right)_{ij} + \sigma\varphi^{(m+1)}_{ij,n+1} + \Gamma_2\varphi^{(m+1)}_{ij,n+1} = \Gamma_2\varphi^{(m)}_{ij,n+1} + F_2,
\end{aligned} \tag{13}$$

where the difference operator $\mathscr{D}_h^2 = \mathscr{D}_x^2 + \mathscr{D}_y^2$, with

$$\begin{aligned}
\mathscr{D}_x^2(\alpha\omega)_{ij} &= \frac{\alpha_{ij}+\alpha_{i+1j}}{2}\frac{\omega_{i+1j}-\omega_{ij}}{h_i^2} - \frac{\alpha_{i-1j}+\alpha_{ij}}{2}\frac{\omega_{ij}-\omega_{i-1j}}{h_i^2},\\
\mathscr{D}_y^2(\alpha\omega)_{ij} &= \frac{\alpha_{ij}+\alpha_{ij+1}}{2}\frac{\omega_{ij+1}-\omega_{ij}}{h_j^2} - \frac{\alpha_{ij-1}+\alpha_{ij}}{2}\frac{\omega_{ij}-\omega_{ij-1}}{h_j^2}.
\end{aligned}$$

$F_1 = \frac{R\rho}{(\gamma-1)}T_{ij,n} + \frac{\Delta t}{2}(\mathscr{D}_h^2(\lambda T_n)_{ij} - \sigma(4\pi B(T^{(m)}_{ij,n+1}) + 4\pi B(T_{ij,n}) - \varphi_{ij,n} - \varphi^{(m)}_{ij,n+1}))$,
$F_2 = \sigma 4\pi B(T^{(m)}_{ij,n+1})$ and Γ_1, Γ_2 are nonnegative monotone terms choosing at each time step t_n such that

$$\Gamma_1 = \max_{ij}\left\{-\frac{\partial F_1}{\partial T}(T_{ij,n},\varphi_{ij,n})\right\}, \quad \Gamma_2 = \max_{ij}\left\{-\frac{\partial F_2}{\partial\varphi}(T_{ij,n},\varphi_{ij,n})\right\}.$$

To compute (T_{n+1}, φ_{n+1}) from (13) one has to solve a linear system of equations of the form

$$\begin{pmatrix} \mathbf{A} + \left(\dfrac{R\rho}{\gamma - 1} + \Gamma_1\right)\mathbf{I} & \mathbf{0} \\ \mathbf{0} & \mathbf{B} + (\sigma + \Gamma_2)\mathbf{I} \end{pmatrix} \begin{pmatrix} T_{n+1}^{(m+1)} \\ \varphi_{n+1}^{(m+1)} \end{pmatrix} = \begin{pmatrix} \Gamma_1 T_{n+1}^{(m)} + F_1 \\ \Gamma_2 \varphi_{n+1}^{(m)} + F_2 \end{pmatrix}, \tag{14}$$

$m = 0, 1, \ldots$, where $\mathbf{A}$ and $\mathbf{B}$ are band-matrices generated by the difference operator $\mathscr{D}_h^2$ for T and φ, respectively.

We now turn our attention to the $\mathscr{M}_1$ model. The first equation in (8) can be solved in similar way as in (13), and the remainder equations can be written in vector form as

$$\partial_x \mathscr{F}(\mathscr{U}) + \partial_y \mathscr{G}(\mathscr{U}) = -\sigma \mathscr{U} + \mathscr{S}(T), \tag{15}$$

$$\mathscr{U} = \begin{pmatrix} \varphi \\ \Psi_1 \\ \Psi_2 \end{pmatrix}, \quad \mathscr{F}(\mathscr{U}) = \begin{pmatrix} \Psi_1 \\ D_{11}\varphi \\ D_{21}\varphi \end{pmatrix}, \quad \mathscr{G}(\mathscr{U}) = \begin{pmatrix} \Psi_2 \\ D_{12}\varphi \\ D_{22}\varphi \end{pmatrix}, \quad \mathscr{S}(T) = \begin{pmatrix} \sigma 4\pi B(T) \\ 0 \\ 0 \end{pmatrix}.$$

D_{ij} $(i, j = 1, 2)$ are the entries of the Eddington matrix $\mathbf{D}$. Assuming the use of the space discretization introduced in the hydrodynamic procedure, the discrete form of (15) reads

$$\mathscr{D}_x \mathscr{V}_{ij}|_{\mathscr{V}_{ij} = \mathscr{F}(\mathscr{U}_{ij})} + \mathscr{D}_y \mathscr{W}_{ij}|_{\mathscr{W}_{ij} = \mathscr{G}(\mathscr{U}_{ij})} + \sigma \mathscr{U}_{ij} = \mathscr{S}(T_{ij}). \tag{16}$$

The difference operators $\mathscr{D}_x$ and $\mathscr{D}_y$ are given in (9). Linearizing the fluxes in (16) and iterating lead to the following radiative algorithm for the $\mathscr{M}_1$ model

$$\begin{aligned} &\mathbf{A} T_{n+1}^{(m+1)} + \left(\frac{R\rho}{\gamma - 1} + \Gamma_1\right) T_{n+1}^{(m+1)} = \Gamma_1 T_{n+1}^{(m)} + F_1(T_{n+1}^{(m)}, \varphi^{(m)}), \\ &(\mathscr{A}^{(m)} + \mathscr{B}^{(m)})\mathscr{U}^{(m+1)} + \sigma \mathscr{U}^{(m+1)} = -\mathscr{D}_x \mathscr{V}^{(m)} - \mathscr{D}_y \mathscr{W}^{(m)} \\ &\qquad\qquad + (\mathscr{A}^{(m)} + \mathscr{B}^{(m)})\mathscr{U}^{(m)} + \mathscr{S}(T_{n+1}^{(m)}), \end{aligned} \tag{17}$$

where the Jacobian matrices $\mathscr{A}$ and $\mathscr{B}$ are given by

$$\begin{pmatrix} 0 & 1 & 0 \\ D_{11} + (\frac{\partial D_{11}}{\partial \varphi})\varphi & (\frac{\partial D_{11}}{\partial \Psi_1})\varphi & (\frac{\partial D_{11}}{\partial \Psi_2})\varphi \\ D_{21} + (\frac{\partial D_{21}}{\partial \varphi})\varphi & (\frac{\partial D_{21}}{\partial \Psi_1})\varphi & (\frac{\partial D_{21}}{\partial \Psi_2})\varphi \end{pmatrix} \quad \text{and} \quad \begin{pmatrix} 0 & 0 & 1 \\ D_{12} + (\frac{\partial D_{12}}{\partial \varphi})\varphi & (\frac{\partial D_{12}}{\partial \Psi_1})\varphi & (\frac{\partial D_{12}}{\partial \Psi_2})\varphi \\ D_{22} + (\frac{\partial D_{22}}{\partial \varphi})\varphi & (\frac{\partial D_{22}}{\partial \Psi_1})\varphi & (\frac{\partial D_{22}}{\partial \Psi_2})\varphi \end{pmatrix},$$

respectively. Once again to compute the solution $(T_{n+1}, \mathscr{U}_{n+1})$ from (17) requires the inversion of a large sparse banded matrix of the form

$$\begin{pmatrix} \mathbf{A} + \left(\dfrac{R\rho}{\gamma - 1} + \Gamma_1\right)\mathbf{I} & \mathbf{0} \\ \mathbf{0} & \tilde{\mathbf{B}} + \sigma \mathbf{I} \end{pmatrix} \begin{pmatrix} T_{n+1}^{(m+1)} \\ \mathscr{U}^{(m+1)} \end{pmatrix} = \begin{pmatrix} \Gamma_1 T_{n+1}^{(m)} + \mathscr{F}_1 \\ \tilde{\mathbf{B}} \mathscr{U}^{(m)} + \tilde{\mathscr{F}}_2 \end{pmatrix}, \tag{18}$$

$m = 0, 1, \ldots$, with $\tilde{\mathbf{B}} = \mathscr{A}^{(m)} + \mathscr{B}^{(m)}$ and $\tilde{\mathscr{F}}_2 = -\mathscr{D}_x \mathscr{V}^{(m)} - \mathscr{D}_y \mathscr{W}^{(m)} + \mathscr{S}(T_{n+1}^{(m)})$. Note that each iteration in the $\mathscr{P}_1$ or $\mathscr{M}_1$ radiative stage requires the solution of a linear system involving a block tridiagonal matrix. The resulting solution process is much more economical than the Newton algorithm in terms of computer storage and CPU time. We would like to point out that another way to solve the equations (15) is to introduce a time marching procedure. Then the methods (10)–(11) remain suitable to compute the required steady state solution provided the size of the time step is restricted such that the radiative signal propagate no more than one grid cell.

As indicated above, all the methods used for space and time discretizations in hydrodynamics and radiation procedures are second order accurate: In hydrodynamics step, the second order MUSCL [8] and second order Runge–Kutta [1] were used, while radiation step employed second order central differencing and second order Crank-Nicolson method. In order to link these procedures in a splitting algorithm which conserves second order accuracy we have used in our numerical experiments the second order accurate Strang splitting [12].

5. Applications

In this section two numerical tests are presented to validate the procedures discussed in previous sections, as well as to compare the $\mathscr{P}_1$ results to those obtained by $\mathscr{M}_1$ computations. Here, the resulting linear system of algebraic equations from (14) or (18) is solved using the preconditioned BI-CGSTAB [13] with a convergence criteria of 10^{-5}. Furthermore, in all the computation runs we set the heat conductivity $\lambda = 10^{-1}$ and the time step $\Delta t = 10^{-3}$. The two-dimensional example is the interaction between a wind and denser cloud [3]. The computational domain is a rectangle of length 2 and height 1 divided into 200×100 grid cells. The initial ambient gas domain has the state $\mathbf{U} = (1, 0, 0, 0.09)^{\mathrm{T}}$ and $T = 0.09$, then a circular cloud of radius 0.15 which is 100 times denser than the gas state is centred at $(0.3, 0.5)$ in the rectangle. The wind is introduced through the left boundary, at which Dirichlet condition is imposed as $\mathbf{U} = (1.5, 6, 0, 30)^{\mathrm{T}}$ and $T = 2$. Outflow condition is applied along the remainder boundaries. The absorption coefficient σ is fixed to 10 in the pre-front of the cloud and 0.1 in the post-front. Fig. 1 shows the numerical results for $\mathscr{P}_1$ and $\mathscr{M}_1$ models at $t = 0.5$. It is apparent that the density and the temperature structures are similar for both models. However, the corresponding norm of the normalized fluxes are totally different. A comparison between $\|\tilde{f}_{\mathscr{P}_1}\|$ and $\|\tilde{f}_{\mathscr{M}_1}\|$ at $x = 0.45$ is reported in the Fig. 2. It is obvious that the flux $f_{\mathscr{M}_1}$ is limited by the speed of light, this condition is not satisfied by the flux $f_{\mathscr{P}_1}$. Furthermore, the density and temperature plots in Fig. 1 compare well with those presented in [3,4]. Our numerical procedures capture the shock and resolve the correct solution well.

The next three-dimensional example is the shock propagation in a unit cube with a centred and highly opaque tube involving incoming flow and thermal source on the front boundary Γ_{int} as showed in Fig. 3(a). Initially the ambient gas in the cube has the state $\mathbf{U} = (1, 0, 0, 300)^{\mathrm{T}}$ and $T = 300$. The boundary state at Γ_{int} is set to $\mathbf{U} = (1.5, 0, 100, 9000)^{\mathrm{T}}$ and $T = 1000$, homogeneous Neumann boundary are used on other boundaries and the velocities u_1 and u_2 vanish on Γ_{ext}. The absorption coefficient σ is fixed to 1000 in the tube and 0.001 otherwise, and we used $50 \times 50 \times 50$ gridpoints. These gridpoints are refined by half in the opaque tube. In Fig. 4 we

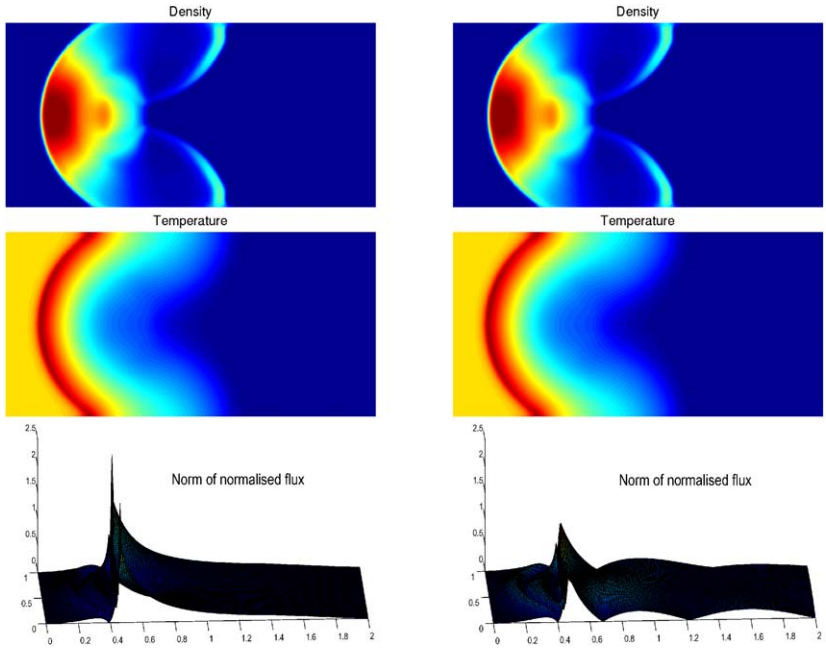

Fig. 1. Density, temperature and norm of normalized flux at $t=0.5$ for the $\mathscr{P}_1$ model (left column) and $\mathscr{M}_1$ model (right column).

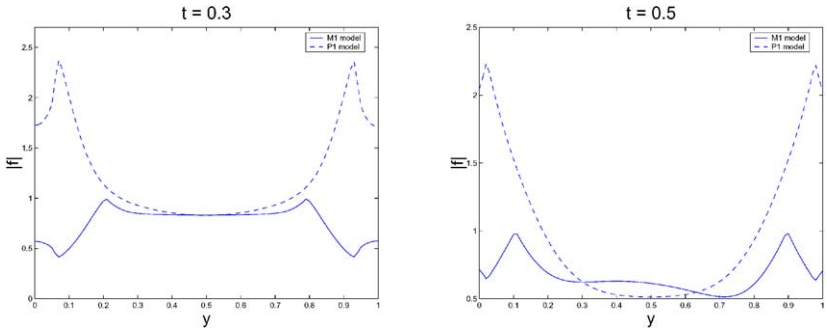

Fig. 2. A cross section of $\|\tilde{f}_{\mathscr{P}_1}\|$ and $\|\tilde{f}_{\mathscr{M}_1}\|$ at $x=0.45$ for two different instants.

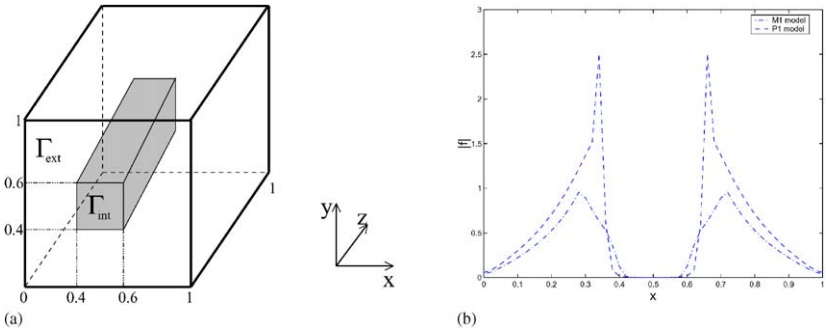

Fig. 3. (a) Geometry of the cube with an opaque tube. The opacity σ is set to 1000 in the tube and 0.001 otherwise. (b) A cross section of $\|\tilde{f}_{\mathscr{P}_1}\|$ and $\|\tilde{f}_{\mathscr{M}_1}\|$ at $z=0.5,\ y=0.2$.

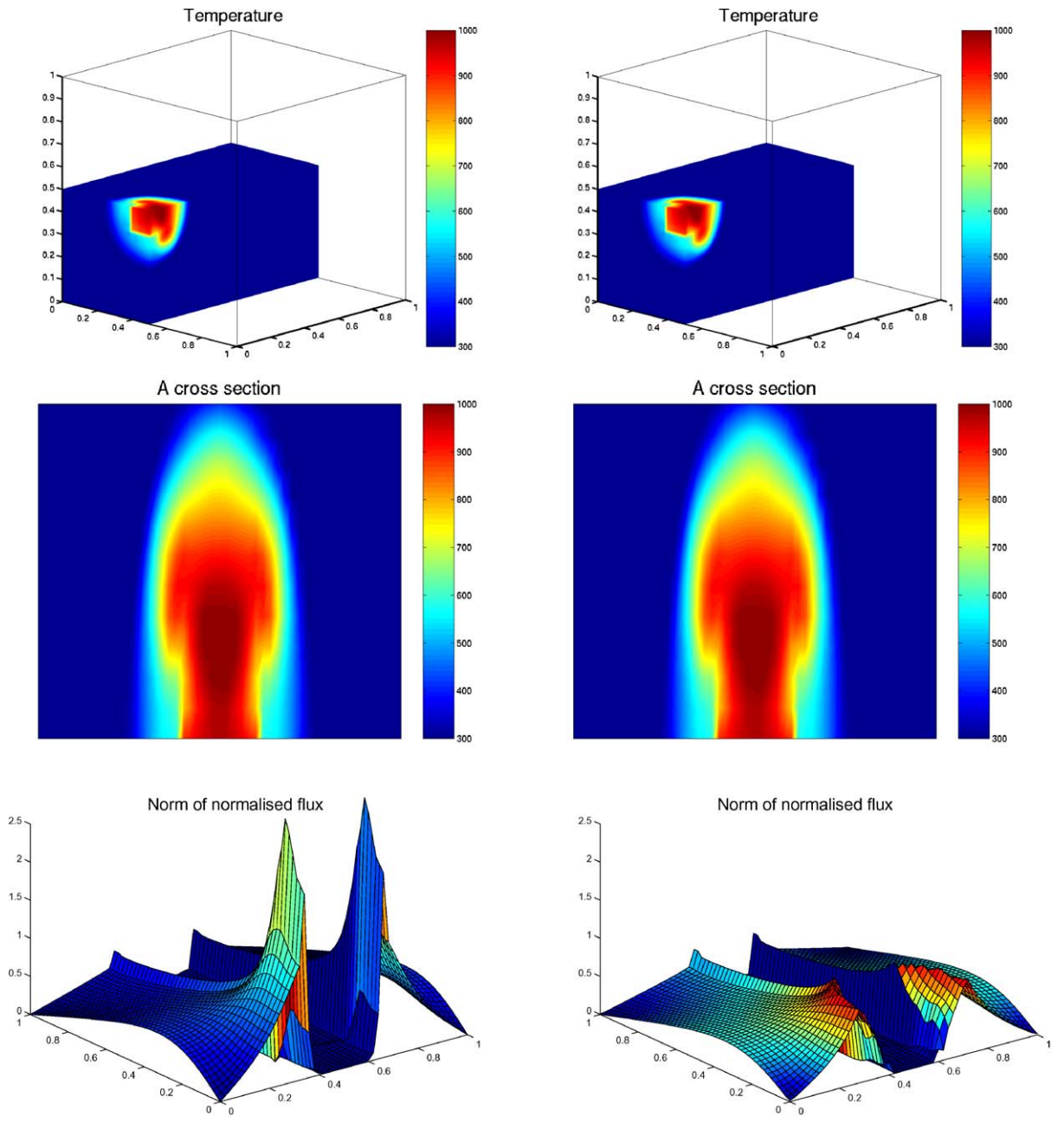

Fig. 4. Temperature, a cross section of the temperature and norm of normalized flux at $z = 0.5$ for the $\mathscr{P}_1$ model (left column) and $\mathscr{M}_1$ model (right column).

report the temperature propagation in the cube as well as a cross section of the temperature and the norm of normalized norm fluxes at $t = 0.1$. Only a part of the computational domain is shown. The profile of the norms $\|\tilde{f}_{\mathscr{P}_1}\|$ and $\|\tilde{f}_{\mathscr{M}_1}\|$ at $z = 0.5, y = 0.2$ is displayed in Fig. 3(b). As we have

pointed out in the previous example, no difference between the temperature patterns in both models. However, regarding to the fluxes $f_{\mathscr{P}_1}$ and $f_{\mathscr{M}_1}$ in Figs. 4 and 3(b), the obtained results are different.

6. Conclusion

We have proposed two approaches for the multidimensional radiation hydrodynamic problems along with numerical algorithm to compute their solutions. The new algorithm consists on splitting the problem in two sets of equations. The set of hydrodynamical equations is approximated by a nonoscillatory relaxation scheme without using neither Riemann solvers nor solving nonlinear systems, while the set of radiative equations is iteratively solved through a monotone Crank-Nicolson method. Numerical experiments have been carried out on two examples, and upon the results obtained we would like to mention that coupling the hydrodynamics to the M_1 model which based on entropy principles has flux limited by the light speed. This property is not preserved by the P_1 model which is based on asymptotic approach, it generates numerical solutions even the radiative flux is above the light speed. Nevertheless to say that, in an opaque medium with constant absorption coefficient, the P_1 approximation can be more efficient and more accurate than Rosseland approach for the hydrodynamic radiation problems.

The multidimensional algorithms presented in this paper can be highly optimized for vector computers, because they are explicit procedures for the first stage and contain no recursive elements neither nonlinear systems in the second stage.

References

[1] W. Bao, S. Jin, High-order I-stable centred difference schemes for viscous compressible flows, J. Comp. Math. 21 (2003) 101–112.
[2] G. Cox, Combustion Fundamentals of Fires, Academic Press, New York, 1995.
[3] W. Dai, P. Woodward, Numerical simulations for radiation hydrodynamics: I. Diffusion limit, J. Comp. Phys. 142 (1998) 182–207.
[4] W. Dai, P. Woodward, Numerical simulations for radiation hydrodynamics: II. Transport limit, J. Comp. Phys. 157 (2000) 199–233.
[5] B. Dubroca, J.I. Feugeas, Entropic moment closure hierarchy for the radiative transfer equation, Preprint.
[6] S. Jin, Z. Xin, The relaxation schemes for systems of conservation laws in arbitrary space dimensions, Comm. Pure Appl. Math. 48 (1995) 235–276.
[7] E. Larsen, G. Thömmes, A. Klar, M. Seaïd, Th. Götz, Simplified P_N approximations to the equations of radiative heat transfer and applications, J. Comp. Phys. 183 (2002) 652–675.
[8] B. van Leer, Towards the ultimate conservative difference schemes V. A second-order sequal to Godunov's method, J. Comp. Phys. 32 (1979) 101–136.
[9] D. Levermore, Relating eddington factors to flux limiters, J. Quant. Spectrosc. Radiat. Trans. 31 (1984) 149–160.
[10] D. Mihalas, B.S. Mihalas, Foundations of Radiation Hydrodynamics, Oxford University Press, New York, 1983.
[11] C. Pao, Numerical methods for coupled systems of nonlinear parabolic boundary value problems, J. Math. Anal. 151 (1990) 581–608.
[12] G. Strang, On the construction and the comparison of difference schemes, SIAM J. Numer. Anal. 5 (1968) 506–517.
[13] H.A. van der Vorst, BI-CGSTAB: A fast and smoothly converging variant of BI-CG for the solution of nonsymmetric linear systems, SIAM J. Sci. Statist. Comp. 13 (1992) 631–644.